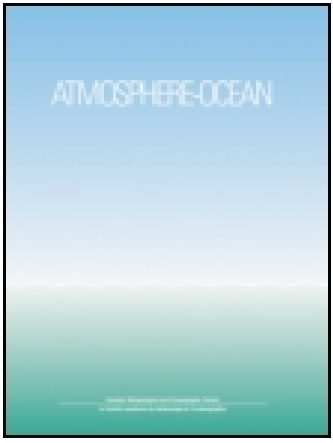

Atmosphere-Ocean
Publication details, including instructions for authors and subscription information:
http://www.tandfonline.com/loi/tato20

The impact of el Nino-Southern oscillation on the temperature field over Canada: Research note

Amir Shabbar [a] & Madhav Khandekar [a]
[a] Atmospheric Environment Service, Environment Canada , 4905 Dufferin Street, Downsview, Ontario, Canada , M3H 5T4
Published online: 19 Nov 2010.

To cite this article: Amir Shabbar & Madhav Khandekar (1996) The impact of el Nino-Southern oscillation on the temperature field over Canada: Research note, Atmosphere-Ocean, 34:2, 401-416, DOI: 10.1080/07055900.1996.9649570

To link to this article: http://dx.doi.org/10.1080/07055900.1996.9649570

The Impact of El Nino-Southern Oscillation on the Temperature Field over Canada

RESEARCH NOTE

Amir Shabbar and Madhav Khandekar
Atmospheric Environment Service, Environment Canada
4905 Dufferin Street
Downsview, Ontario, Canada M3H 5T4

[Original manuscript received 28 July 1995; in revised form 16 November 1995]

ABSTRACT *The impact of the two phases of El Niño-Southern Oscillation (ENSO), namely El Niño and La Niña, on the surface and lower tropospheric temperature fields over Canada is documented. Gridded surface temperature data for 91 years (1900–1990) and 500–1000 hPa thickness data for 49 years (1946–1994) have been analyzed statistically in the context of El Niño, La Niña and normal years.*

Using a composite analysis, the present study conclusively demonstrates that significant positive surface temperature anomalies spread eastward from the west coast of Canada to the Labrador coast from the late fall to early spring (November through May) following the onset of El Niño episodes. The accompanying temperatures in the lower troposphere show a transition from the Pacific/North American (PNA) pattern to the Tropical/Northern Hemisphere (TNH) pattern over the North American sector during the same period. Conversely, significant negative surface temperature anomalies spread southeastward from the Yukon and extend into the upper Great Lakes region by the winter season following the onset of La Niña episodes. Furthermore, the lower tropospheric temperatures show a negatively-phased PNA-like pattern in early winter which weakens considerably by May of the following year. Thus, while western Canadian surface temperatures are influenced during both phases of ENSO, eastern Canadian surface temperature effects are found during the El Niño phase only. The impact of ENSO on the Canadian surface temperatures is the strongest during the winter season and nearly disappears by spring (April and May). The largest positive (negative) anomalies are found to be centred over two separate regions, one over the Yukon and the other just west of Hudson Bay in the El Niño (La Niña) years. Over western Canada, mean wintertime temperature distribution of the El Niño (La Niña) years is found to be shifted towards warmer (colder) values relative to the distribution of the normal years.

This study suggests the possibility of developing a long-range forecasting technique for Canada using ENSO related indices.

RÉSUMÉ *On présente l'impact des deux phases de l'ENSO (El Niño Oscillations australes), à savoir l'El Niño et La Niña, sur les champs des températures à la surface et de la basse atmosphère sur le Canada. La grille des températures à la surface sur 91 ans (1900–1990)*

et des données d'épaisseur 500-1000 hPa sur 49 ans (1946–1994) analysée statistiquement sous le jour de périodes de l'El Niño et de La Niña, et d'années normales.

A l'aide d'une analyse composite, l'étude nous a convaincu que des anomalies positives importantes de la température à la surface se propagent vers l'est, de la côte ouest du Canada à celle du Labrador, de tard à l'automne à tôt au printemps (de novembre à mai) à la suite d'épisodes de l'El Niño. Les températures associées de la basse atmosphère présentent une transition de la configuration Pacifique/Amérique du Nord (PNA) à celle de Tropique/Hémisphère Nord (TNH) sur le secteur nord du continent durant la même période. En même temps, des anomalies négatives importantes de la température à la surface se sont propagées vers le sud-est, du Yukon à la région supérieure des Grands Lacs, durant l'hiver suivant les épisodes de La Niña. De plus, les températures de la basse atmosphère montrent une configuration phasée négative semblable à la PNA tôt en hiver qui devient beaucoup plus faible vers mai de l'année suivante. Donc, alors que les températures à la surface sur l'ouest canadien subissent l'influence des deux phases de l'ENSO, les effets sur ces températures sur l'est n'apparaissent que pendant les épisodes de l'El Niño. L'impact de l'ENSO sur les températures à la surface au Canada est plus fort durant l'hiver disparaissant presque complètement au printemps (avril et mai). Les anomalies positives (négatives) les plus grandes sont centrées sur deux régions séparées: sur le Yukon et juste à l'ouest de la baie d'Hudson durant les épisodes de l'El Niño (La Niña). Sur l'ouest, la distribution de la température hivernale moyenne au cours des épisodes de l'El Niño (La Niña) retrouve des valeurs plus chaudes (froides) en relation à la distribution des années normales.

L'étude permet la possibilité d'établir une technique de prévision à long terme pour le Canada utilisant des indices apparentés à l'ENSO.

1 Introduction

An important source of interannual climate variation is the ENSO phenomenon which has been shown to influence weather and climate anomalies over various regions of the world (e.g., Enfield, 1989; Kiladis and Diaz, 1989; Ropelewski and Halpert, 1987). An ENSO episode has been found to have some well-known atmospheric teleconnective patterns with middle latitudes of North and South America (e.g., Horel and Wallace, 1981; Hoskins and Karoly, 1981). During the warm phase of the ENSO episode, the Southern Oscillation index (which is defined as the difference in sea-level pressure between Tahiti and Darwin) is negative, while over the middle latitudes there is a tendency for the Aleutian low pressure centre to be strengthened, higher than normal pressure patterns to be found over western Canada and anomalously low pressure to be located over the southeastern U.S.A. During the cold phase of ENSO, the Southern Oscillation index is positive, the Aleutian low is weaker and a strong high pressure ridge often develops over Alaska and the Yukon. A number of investigators have examined relationships between tropospheric temperatures and the two phases of the Southern Oscillation (Angell, 1981; Pan and Oort, 1983; Halpert and Ropelewski, 1992).

The pervasive impact of ENSO on world-wide weather and climate has also prompted a number of numerical modelling studies to simulate the ENSO phenomenon and related climate anomalies using coupled atmosphere-ocean models (e.g., Zebiak and Cane, 1987; Barnett et al., 1994; Ji et al., 1994). Atmospheric and oceanic parameters associated with various phases of the ENSO phenomenon

can provide valuable guidance for short-term climate prediction in many countries of the Indo-Pacific basin (e.g., Indian monsoon rainfall prediction; seasonal rainfall prediction over some central and south American countries). According to Halpert and Ropelewski (1992), hereafter referred to as HR, the strongest Southern Oscillation-temperature relationships occur in the tropics, with the surface temperature anomalies having the same sign as the local sea-surface temperature anomalies. Outside the tropics, the relationship between the Southern Oscillation and surface temperatures is most likely the result of the tropical forcing of large-scale extratropical circulation patterns, as envisaged in the landmark studies of Bjerknes (1966, 1969).

The impact of ENSO on temperature and precipitation patterns over the U.S.A., as well as over the central and south American countries, has been documented in several recent studies (Ropelweski and Halpert, 1987, 1989; Halpert and Ropelewski, 1992; Pisciottano et al., 1994.) The study by HR suggests that warmer than normal surface temperatures occur over parts of the Canadian western provinces during the mature phase of a warm ENSO episode and that cooler than normal temperatures occur over the same region during the mature phase of a cold ENSO episode; however, their study considers only the large-scale temperature relationships and does not provide details of the ENSO impact on various regions of Canada. Furthermore, for eastern Canadian regions, their analysis is based on a rather limited number of ENSO cases and hence does not fully address the impact of ENSO on eastern Canada (Halpert, Climate Prediction Centre U.S.A. – personal communication).

The purpose of this investigation is to make a comprehensive analysis of the impact of the extreme phases of ENSO, namely El Niño and La Niña, on the surface temperatures over various regions of Canada. Additionally, the response of the tropical forcing on the lower tropospheric air temperatures over Canada is examined. Using two sets of data, as described in Section 2, this study focuses on the evolution of the temperature response from the fall of the ENSO onset year to the spring of the following year over various regions of Canada.

2 Data

The surface dataset used in this study is the combined land and marine gridded monthly surface air temperature anomalies (departure from a 1951–1979 mean). This dataset is an updated version of Jones et. al (1986) surface temperature data and was obtained from the Oak Ridge National Laboratory in the U.S.A. The dataset covers the period 1851 to 1991 on a 5 degree latitude by 10 degree longitude grid of the Northern Hemisphere. Each grid point temperature serves as an average value for all stations nearest to that grid point.

Homogeneity of the data was checked by comparison with data from adjacent stations. The dataset suffers from poor spatial coverage prior to 1900 particularly in the high latitudes and the eastern Canadian Arctic. Data coverage is fairly good after 1900 from the Yukon through western Canada and the Great Lakes basin into the Canadian Maritime provinces. This study focuses on the effects of ENSO from

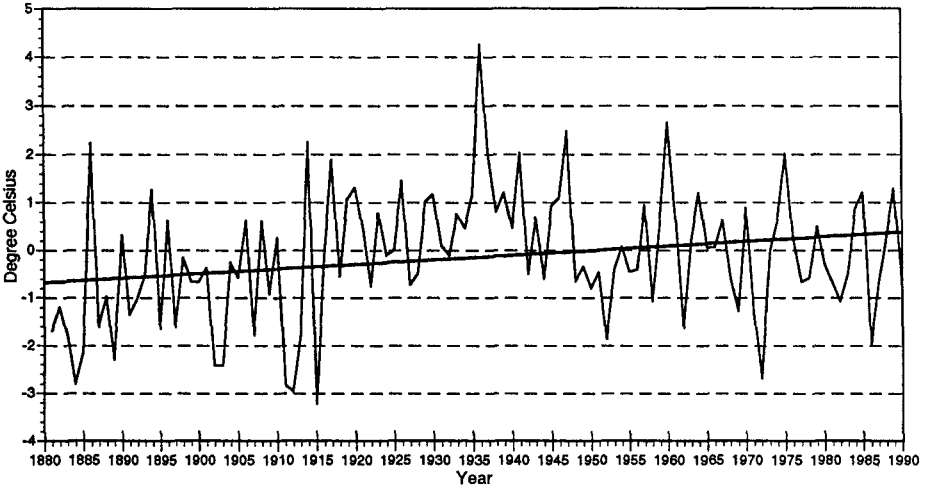

Fig. 1 A typical July temperature trend in western Canada as shown for a grid point in southern Manitoba.

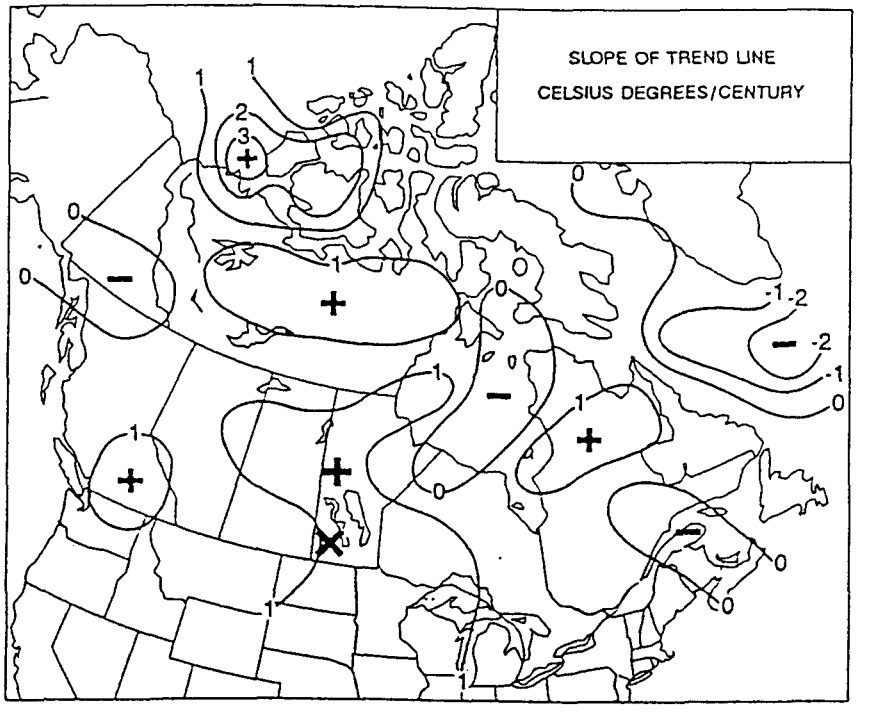

Fig. 2 Isopleths of the slope of the temperature trend line in July (°C/century).

1900 to 1990 (91 years). In order to remove bias in the dataset, a linear trend is removed at each grid point for each month separately. Figure 1 shows a typical trend line for a grid point in southern Manitoba in July. The slopes of the July temperature trend line at different grid locations are shown as isolines in Fig. 2. The slope is positive in western and northern Canada but negative south of Greenland. These findings are in general agreement with those reported by Jones (1988).

The upper air data for this investigation consist of monthly (1200 UTC) 500 and 1000 hPa height analyses of the Northern Hemisphere (15 – 90°N) on a 455 grid point network of 5° latitude by 10° longitude for the period 1946 to 1994. The data from 1946–1981 originated from the National Meteorological Center (NMC) twice daily analyses and were obtained from the National Center for Atmospheric Research (NCAR) (Jenne, 1975). Throughout the dataset there were a few cases of missing data. Interpolation (often from 0000 UTC) was used to estimate height for the missing days (1–2 days). Larger gaps were filled in by digitizing hand drawn analyses obtained from the United States Weather Bureau Historical Map Series. The balance of the data was obtained from the Canadian Meteorological Centre (Shabbar et al., 1990). The 500–1000 hPa anomaly is calculated relative to the 49-year (1946–1994) base period.

3 Analysis method

Horel and Wallace (1981) showed that the circulation anomalies in the extratropics are better related to the sea surface temperatures (SST) in the central Pacific rather than to the SSTs in the eastern Pacific. According to Deser and Wallace (1987), the central Pacific SSTs and the Southern Oscillation index are highly correlated. Therefore in this study, strong to moderate ENSO years have been defined as those years in which the 5-month running mean Southern Oscillation index remained in the lower 25% (El Niño) or upper 25% (La Niña) of the distribution for 5 months or longer. This definition of ENSO is consistent with that chosen by Rasmusson (1984), Ropelewski and Jones (1987) and Halpert and Ropelewski (1992). In this study we examine the effect of 23 strong to moderate El Niño episodes (Table 1) and 17 strong to moderate La Niña episodes (Table 2) on the surface and lower tropospheric temperatures over Canada from the late fall of the ENSO onset year to the spring of the following year. When the warm and the cold phases of the ENSO episode occurred in consecutive years (i.e., 1987 and 1988) or when one phase of ENSO spanned more than one year (i.e., 1957 and 1958), our analysis treated these episodes as independent episodes. Composites of temperatures are computed independently for each phase of ENSO. The composites were obtained by averaging three-month temperatures from all cases; then they were tested for statistical significance. The procedure used for statistical testing is described in Appendix A. The locations where the temperature anomalies are statistically significant are indicated by shading on the surface composite maps (Figs 3 and 5).

TABLE 1. Years of onset of strong to moderate El Niño events from the turn of the century. During these events, the Tahiti-Darwin Southern Oscillation Index remained in the lower 25% of the distribution for 5 months or longer (after Rasmusson, 1984).

1900–09	1910–19	1920–29	1930–39	1940–49	1950–59	1960–69	1970–79	1980–89
1902	1911	1925	1930	1941	1951	1965	1972	1982
1905	1912	1926	1939		1953	1969	1976	1986
	1916	1929			1957			
	1918				1958			
	1919							

TABLE 2. Years of onset of strong to moderate La Niña events from the turn of the century. During these events, the Tahiti-Darwin Southern Oscillation Index remained in the upper 25% of the distribution for 5 months or longer (after Ropelewski and Jones, 1987).

1900–09	1910–19	1920–29	1930–39	1940–49	1950–59	1960–69	1970–79	1980–89
1904	1910	1926	1938	–	1950	1964	1970	1988
1909	1916	1928			1955		1971	
	1917				1956		1973	
							1975	

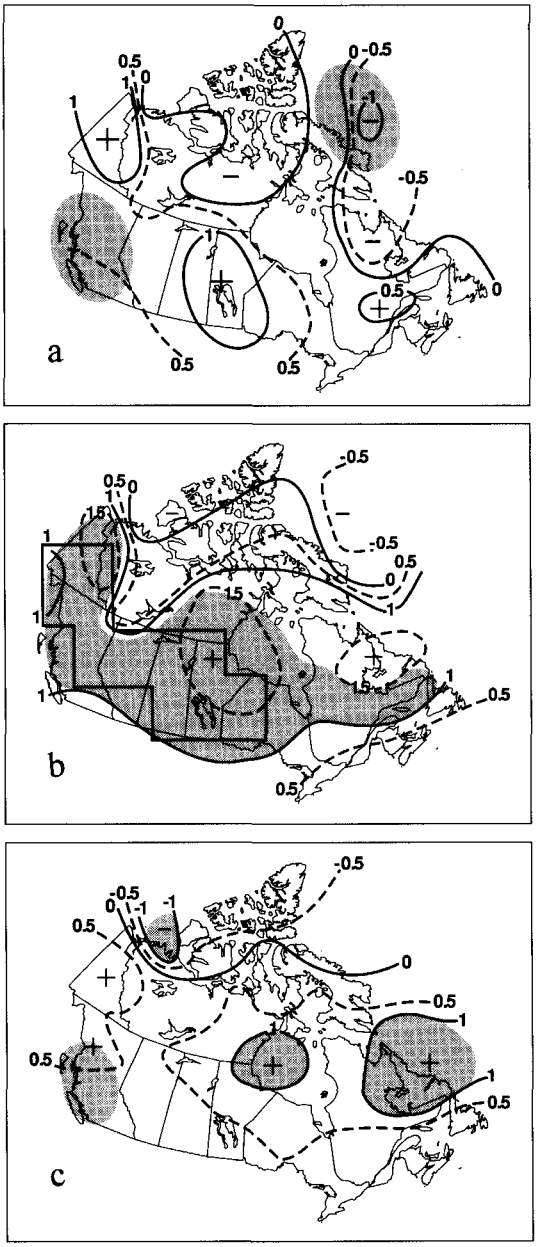

Fig. 3 Mean temperature anomaly composite (°C) of 23 strong to moderate El Niño episodes between 1900 and 1990 (a) Nov–Jan, (b) Jan–Mar and (c) Mar–May. Values in the shaded areas are statistically significant at the 5% level. Values in the boxed area of 3(b) are used to calculate the temperature distribution shown in Fig. 7.

4 Results and discussion

a *El Niño and Canadian Temperature*

The composites of the Canadian surface temperature anomaly patterns for the three-month averages from the fall of the El Niño onset year to the following spring during the 23 years of the warm phase of ENSO, between 1900 and 1990, are shown in Figs 3(a–c). Similar composites of thickness (500–1000) hPa anomaly for three-month averages spanning the months of November to May are presented in Figs 4(a–c). The Nov–Jan composite (Fig. 3a) shows the emergence of above normal temperatures over western Canada. The positive anomalies over British Columbia, as well as the negative anomalies east of Baffin Island, are statistically significant. The corresponding 500–1000 hPa thickness map (Fig. 4a) for the same period shows a pattern which resembles the PNA pattern (Horel and Wallace, 1981; Barnston and Livezey, 1987). The positive anomaly centre over western Canada is indicative of the amplification of the western Canadian ridge, while the negative anomaly centre over the north-eastern Pacific ocean signifies a deepening of the Aleutian Low. The combination of these two features gives rise to a strong southwesterly flow along the west coast of Canada producing positive surface temperature anomalies in British Columbia and extending into central Canada. The positive surface temperature anomaly over western Canada strengthens and expands eastward during the winter months as can be seen in Fig. 3b. A large area of positive temperature anomaly extending from the Yukon in the west to Labrador in the east is evident. Embedded in this large area are three centres, one over the Yukon, one over central Canada and one over Labrador showing a positive anomaly of 1.5°C. The corresponding composite of 500–1000 hPa thickness (Fig. 4b) shows an evolution from the PNA-like pattern to the TNH pattern (Barnston and Livezey, 1987) with a large positive area extending from the Canadian Rockies to Labrador. For the spring months (March–May), surface temperatures and 500–1000 hPa composites are shown in Fig. 3c and Fig. 4c respectively. At the surface level, there is a small and shrinking area of positive temperature anomaly on the west coast while over western and central Canada the ENSO impact appears to have diminished substantially. In the 500–1000 hPa thickness field, a weak positive anomaly centre persists east of Hudson Bay while the anomaly pattern is rather weak over the west coast of Canada.

The results shown in Fig. 3 are in general agreement with those of HR, in which surface temperatures are subjected to harmonic analysis. The first harmonic of the 24-month idealized Southern Oscillation cycle was used in their composites. In general, our results are in agreement with theirs in western Canada. However, there are significant differences in eastern Canada. Whereas HR found a separate warm area over the Canadian Maritime provinces and Newfoundland during winter, we find positive anomalies over eastern Canada as an extension of the western Canadian positive anomalies. In addition, our analysis shows significant positive anomalies over Labrador and not over the Maritime provinces as shown by HR. The difference between our analysis and those of HR could be attributed to a number of reasons. HR only look for large-scale coherent temperature pattern responses to ENSO

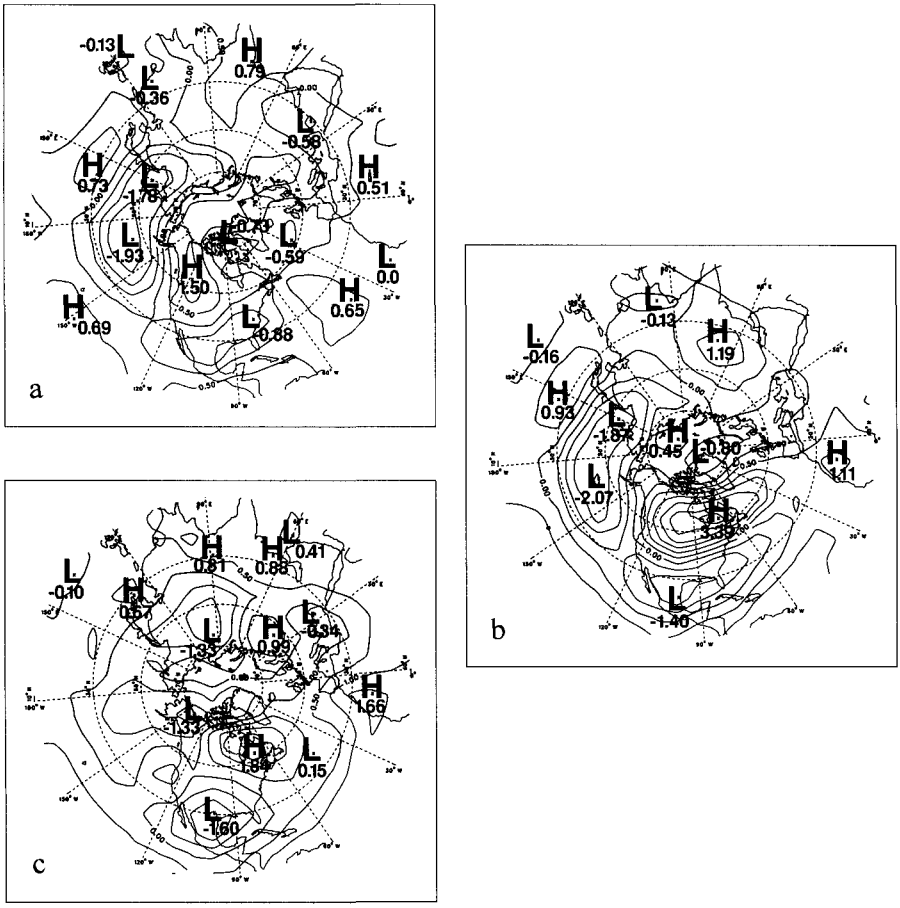

Fig. 4 Mean 500–1000 hPa thickness anomaly composite (dam) of strong to moderate El Niño episodes between 1946 and 1994 (a) Nov–Jan, (b) Jan–Mar and (c) Mar–May.

forcing that last for many months, thus not fully considering isolated stations or localized areas that may possess strong ENSO-temperature relationships. Further, in their study, the composite for each station is fitted to a single 24-month Southern Oscillation, designed to contain a Southern Oscillation effect period. This assumes a general peak or trough during roughly half of that effect period. Due to the temporal smoothing inherent in this technique, short-lived (e.g. 3 to 4 months) but genuine ENSO impact periods might not be detected. Moreover, stations with fewer than five warm and cold ENSO episodes in the record were not included in their analysis. Our analysis is based on a more comprehensive dataset, and examines the evolution of ENSO response in the surface and lower tropospheric temperatures. This approach brings out regional details not previously documented.

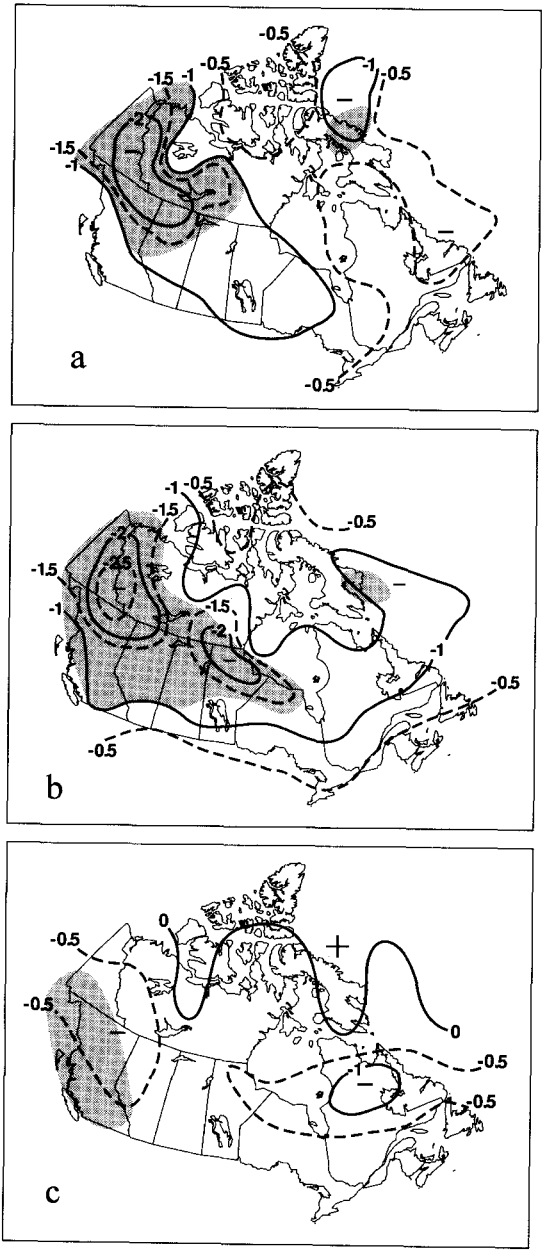

Fig. 5 Mean temperature anomaly composite (°C) of 17 strong to moderate La Niña episodes between 1900 and 1990 (a) Nov–Jan, (b) Jan–Mar and (c) Mar–May. Values in the shaded areas are statistically significant at the 5% level.

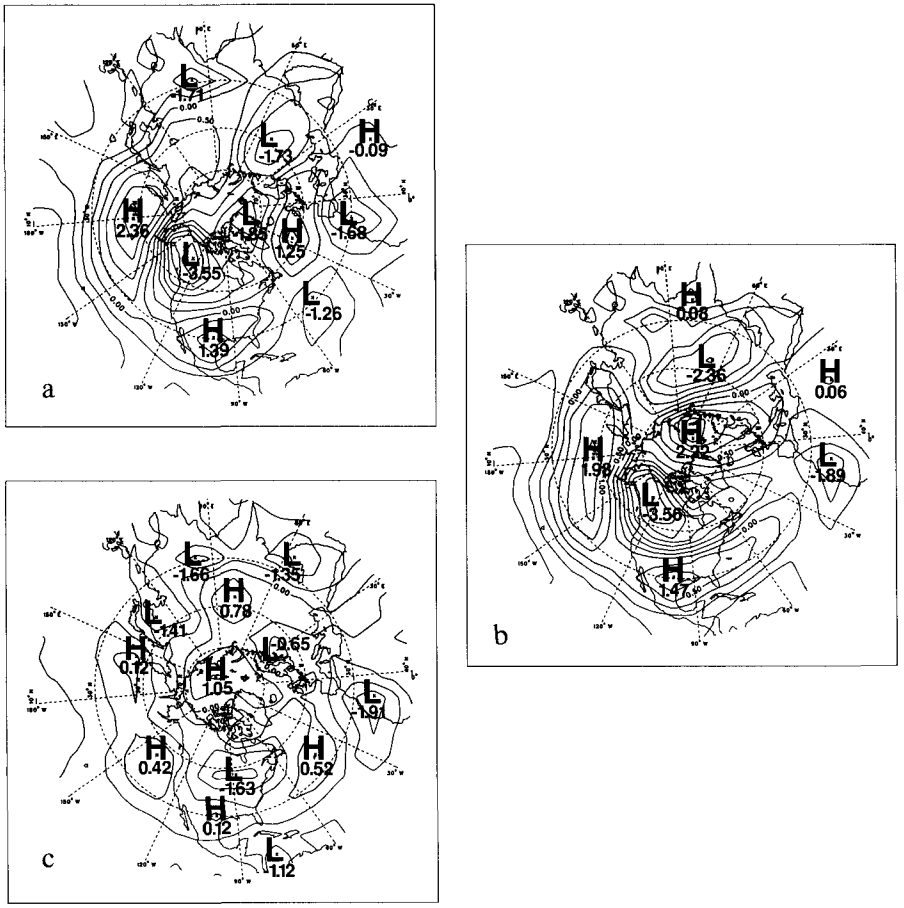

Fig. 6 Mean 500–1000 hPa thickness anomaly composite (dam) of strong to moderate La Niña episodes between 1946 and 1994 (a) Nov–Jan, (b) Jan–Mar and (c) Mar–May.

b *La Niña and Canadian Temperature*

The composites of the Canadian temperature pattern based on 17 cold phases of ENSO covering three-month averages from the fall of the La Niña onset year to the following spring are shown in Figs 5(a–c). The Nov–Jan composite (Fig. 5a) shows significant negative temperature anomalies from the Yukon to the northwestern Canadian prairies. Since there are fewer cold than warm ENSO years (17 cold years versus 23 warm years–this implies that a more extreme tail of the Canadian surface climate distribution is seen for the cold episodes) the cold phase surface temperature anomalies are found to be stronger than the corresponding warm phase anomalies (Fig. 3a). The 500–1000 hPa map (Fig. 6a) for the same period shows a negatively-phased PNA-like pattern over the North American sector. The combination of a

negative anomaly centre over the Canadian Rockies and a positive anomaly centre over the northeastern Pacific ocean is conducive to northwesterly cold air advection over western Canada. This cold advection produces a negative surface temperature anomaly over the Yukon and northern British Columbia which spreads into central Canada as shown in Fig. 5a. In addition, a small negative anomaly centre appears in the northwestern Atlantic over the Davis Strait.

During the next two time periods (Jan–Mar and Mar–May), the composite patterns (Figs 5(b–c)) show two separate areas of strong negative anomaly centres, one over the Mackenzie Valley and the other over the regions just west of Hudson Bay. In contrast to the warm phase composite, however, negative surface temperature anomalies remain confined mainly to western Canada during the winter months. The corresponding 500–1000 hPa map (Fig. 6b) shows a negatively-phased PNA-like pattern which weakens considerably by spring (Mar–May) (Fig. 6c). Both surface and 500–1000 hPa negative anomalies weaken considerably during the Mar–May period, and by early summer no ENSO related anomalies are found over Canada. Western Canada exhibits ENSO-temperature relationships during both phases of ENSO and is opposite in sign, i.e., positive temperature anomalies predominate in the warm phase and negative temperature anomalies are mainly evident during the cold phase of ENSO. Eastern Canada, however, appears to show the ENSO influence only in the warm phase. In this study, a statistical test of differences in correlation (Canadian surface temperatures versus Southern Oscillation index) between the two ENSO phases has not been evaluated. This test, through Monte Carlo simulations, will be carried out in subsequent studies when regional and individual ENSO response will be investigated in more detail.

c *Variability in Relationship*

A composite of the mean temperature anomaly distribution for El Niño, La Niña and normal years in western Canada is shown in Fig. 7. The values shown are the average of all the grid points in the boxed area as shown in Fig. 3b during the Jan–Mar period. A Guassian curve is fitted to the three distributions separately. It is clear that the mean of the distribution of the El Niño temperatures is shifted towards the warmer temperatures relative to the normal temperature distribution and the distribution of the La Niña temperatures is shifted towards the colder temperatures relative to the normal temperature distribution. It may be noted that some El Niño winters have been associated with temperatures which are colder than the normal winters and some La Niña winters have been associated with temperatures which are warmer than the normal winters. Even though the means of the El Niño and La Niña temperatures distributions are statistically different from the normal distribution at the 5% level, there is considerable overlap among the three distributions. The maximum and minimum of the average of all the grid points in the boxed area in Fig. 3b from the ENSO onset year to the following year are shown in Table 3. The range of temperature response is rather large (~5°C) for both phases of ENSO in western Canada. The variability among the warm

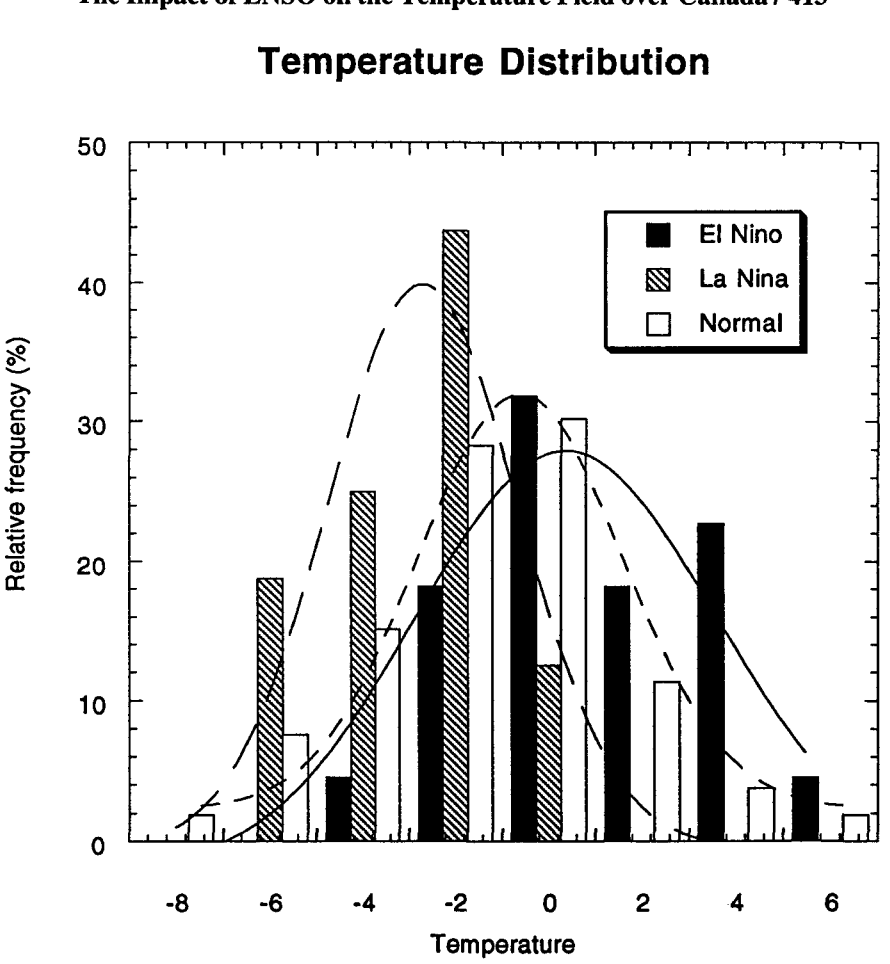

Fig. 7 Mean temperature anomaly distribution for El Niño (solid), La Niña (hatched) and normal (open) years for the boxed area shown in Fig. 3(b). Note a definite shift toward warmer (cooler) values during the El Niño (La Niña) years. A Guassian curve is fitted separately to the three distributions.

episodes or among cold episodes is quite large, despite the statistical significance of the differences in their means from the climatological means. This implies that the predictive skill, given a knowledge of the ENSO state, would not be especially high even though it would most likely be at a usable level, i.e., correlation of about 0.5.

5 Summary and concluding remarks

This paper appraises the reality and nature of ENSO influence on the Canadian climate in time and space by examining the detailed response of surface temper-

TABLE 3. Maximum and minimum monthly mean temperature anomaly (°C) following the 23 El Niño and 17 La Niña events for the grid points in the boxed area of Fig. 3b.

	El Niño		La Niña	
	Max	Min	Max	Min
Nov–Jan	4.2	−2.3	2.5	−4.8
Dec–Feb	5.3	−0.1	1.2	−3.9
Jan–Mar	5.5	1.4	2.3	−3.1
Feb–Apr	4.2	−2.3	2.5	−4.8
Mar–May	3.3	−1.9	2.4	−1.6

atures and 500–1000 hPa thickness fields to the two phases of ENSO. For the warm phase, we find that significant positive temperature anomalies first appear in western Canada and then expand eastward during the winter months. The temperature response in the lower troposphere is consistent with the presence of the PNA and TNH patterns.

The composites of 23 years of the warm phase of the ENSO phenomenon show significant warmth from the fall of the El Niño onset year to the following spring from the Yukon through the Prairies and into the Labrador coast. By summer (i.e., about 8 to 10 months after the onset of El Niño) significant temperature anomalies completely disappear from most regions of Canada. In addition, the 500–1000 hPa thickness pattern shows a transition from the PNA pattern in early winter to the TNH pattern by the following late winter through early spring.

The composites of 17 years of the cold phase of the ENSO phenomenon show temperatures significantly below normal in western Canada. The Dec–Feb pattern (not shown) represents the farthest eastward progression of significantly cold anomalies reaching north of the Great Lakes region. The negative anomalies remain confined mainly to the Canadian prairies, British Columbia and the Yukon during the cold phase of ENSO. While the western regions of Canada exhibit temperature changes during both phases of ENSO, eastern Canada shows temperature changes only during the warm phase of ENSO. The largest positive (negative) anomalies are found to be centred over two separate regions, one over the Yukon and the other just west of Hudson Bay in the El Niño (La Niña) years.

The mean temperature distribution for the warm (cold) phase of ENSO shows a significant shift towards warmer (cooler) values, especially for locations in western Canada. Although El Niño and La Niña episodes have been shown to influence the mean Canadian surface temperature patterns significantly, as revealed by Fig. 7, the impact of individual El Niño and La Niña episodes varies markedly and hence the above findings can only be used as a general guideline. Further investigation is necessary to determine the impact of El Niño and La Niña on interannual variability of the Canadian climate. Recent studies by Graham and Barnett (1995) and Barnston (1994) have clearly demonstrated the utility of the equatorial SST for long-range

prediction of extratropical climate anomalies with a lead time of six months or more. The results shown here strongly motivate us to use ENSO related indices for developing long-range forecasting techniques for Canada; this work is in progress and will be reported on in the near future.

Acknowledgements

The authors wish to thank Drs. Kaz Higuchi and John Knox of the Atmospheric Environment Service for providing helpful comments and suggestions. We also appreciate the useful comments of the anonymous reviewers.

Appendix

The statistical significance of the composites is investigated by the use of the Student t-test (Norman and Streiner, 1986). If $\bar{T}_1$ represents the seasonal average temperature anomaly for the El Niño years (23 cases) and $\bar{T}_2$ represents a similar average for the normal years (53 cases), then the t-statistic is given by

$$t = \frac{\bar{T}_1 - \bar{T}_2}{s\sqrt{\frac{1}{n_1} + \frac{1}{n_2}}} \tag{1}$$

where s^2 is the sample variance given by

$$s^2 = \frac{\sum_1^{n_1}(T_1 - \bar{T}_1)^2 + \sum_1^{n_2}(T_2 - \bar{T}_2)^2}{n_1 + n_2 - 2} \tag{2}$$

In (1) and (2), $n_1 = 23$, $n_2 = 53$ and the overbar quantity represents the average value over the number of cases. The t-test is designed to assess the significant difference between the two means (mean for El Niño years versus mean for normal years). The shaded area in Fig. 3b, for example, shows the region where the t-statistic is significant at the 5% level of significance. Similar tests are performed for other three-month average composites (Figs 3 and 5) and the locations where the temperature anomalies are statistically significant are indicated by shading.

References

ANGELL, J.K. 1981. Comparison of variations in atmospheric quantities with sea surface temperature variations in the equatorial eastern Pacific. *Mon. Weather Rev.* **109**: 230–243.

BARNETT, T.P.; L. BENGTSSON, K. ARPE, M. FLUGEL, N. GRAHAM, M. LATIF, J. RITCHIE, E. ROECKNER, U. SCHLESE, U. SCHULZWEIDA and M. TYREE. 1994. Forecasting global ENSO-related anomalies. *Tellus*, **46A(4)**: 381–394.

BARNSTON, A.G. and R.E. LIVEZEY, 1987. Classification, seasonality and persistence of low-frequency circulation patterns. *Mon. Weather Rev.* **115**: 1083–1126.

———. 1994. Linear statistical short-term climate predictive skill in the Northern Hemisphere. *J. Clim.* **7**: 1513–1564.

BJERKNES, J. 1966. A possible response of the atmospheric Hadley circulation to equatorial

anomalies of ocean temperature. *Tellus*, **18**: 820–829.

———. 1969. Atmospheric teleconnections from the equatorial Pacific. *Mon. Weather Rev.* **97**: 163–172.

DESER, C. and J.M. WALLACE. 1987. El Niño events and their relation to the Southern Oscillation: 1925–1986. *J. Geophys. Res.* **92**: 14 189–14 197.

ENFIELD, D.B. 1989. El Niño, past and present. *Rev. Geophys.* **27(1)**: 159–187.

GRAHAM, N.E. and T.P. BARNETT. 1995. ENSO and ENSO-related predictability. Part II: Northern Hemisphere 700-mb height prediction based on a hybrid coupled ENSO model. *J. Clim.* **8**: 544–549.

HALPERT, M.S. and C.F. ROPELEWSKI. 1992. Surface temperature patterns associated with the Southern Oscillation. *J. Clim.* **5**: 577–593.

HOREL, J.D. and J.M. WALLACE. 1981. Planetary scale atmospheric phenomena associated with the Southern Oscillation. *Mon. Weather Rev.* **109**: 813–829.

HOSKINS, B.J. and D.J. KAROLY. 1981. The steady linear response of a spherical atmosphere to thermal and orographic forcing. *J. Atmos. Sci.* **38**: 1179–1196.

JENNE, R. 1975. Data sets for meteorological research. NCAR-TN/JA111, 194 pp.

JI, M; A. KUMAR and A. LEETMAA. 1994. An experimental coupled forecast system at the National Meteorological Center: Some early results. *Tellus*, **46A**: 398–418.

JONES, P.D.; S.C.B. RAPER, R.S. BRADLEY, H.F. DIAZ, P.M. KELLY and T.M.L. WIGLEY. 1986. Northern Hemisphere surface air temperature variations, 1851–1984. *J. Clim. Appl. Meteorol.* **25**: 161–179

———. 1988. Hemispheric surface air temperature variations: Recent trends and an update to 1987. *J. Clim.* **1**: 654–660.

KILADIS, G.N. and H.F. DIAZ. 1989. Global climate anomalies associated with extremes in the Southern Oscillation. *J. Clim.* **2**: 1069–1090.

NORMAN, G.R. and D.L. STREINER. 1986. *PDQ Statistics*. B.C. Decker Inc. pp. 41–45.

PAN, Y.H. and A.H. OORT. 1983. Global climate variations connected with sea surface temperature anomalies in the eastern equatorial Pacific Ocean for the 1958–73 period. *Mon. Weather Rev.* **111**: 1244–1258.

PISCIOTTANO, G.; A. DIAZ, G. CAZAS and C.R. MECHOLO. 1994. El Niño-Southern Oscillation impact on rainfall in Uruguay. *J. Clim.* **7**: 1286–1302.

RASMUSSON, E.M. 1984. El Niño: The ocean/atmosphere connection. *Oceanus*, **27, No. 2:** 5–12.

ROPELEWSKI, C.F. and M.S. HALPERT. 1987. Global and regional scale precipitation patterns associated with El Niño/Southern Oscillation. *Mon. Weather Rev.* **115:** 1606–1626.

——— and ———. 1989. Precipitation patterns associated with the high index phase of the Southern Oscillation. *J. Clim.* **2**: 268–284.

——— and P.D. JONES. 1987. An extension of the Tahiti–Darwin Southern Oscillation index. *Mon. Weather Rev.* **115:** 2161–2165.

SHABBAR, A.; K. HIGUCHI and J.L. KNOX. 1990. Regional analysis of Northern Hemisphere 50 kPa geopotential heights from 1946 to 1985. *J. Clim.* **3:** 543–557.

ZEBIAK, S.E. and M.A. CANE. 1987. A Model El Niño-Southern Oscillation. *Mon. Weather Rev.* **115**: 2262–2278.